Muon Acceleration in a 'Dogbone' RLA – Beam Dynamics Issues

S. Alex Bogacz
Center for Advanced Studies of Accelerators
Jefferson Lab, Newport News, Virginia

Introduction – Overall Acceleration Scenario

To ensure adequate survival rates of short-lived muons, acceleration must occur at high average gradient. Initial estimate [1] shows that an RF gradient of 15 MV/m will allow survival of about 85% of source muons throughout the RLA complex. Since muons are generated as a secondary beam they occupy large phase-space volume [2]. The accelerator must provide high average gradient, while maintaining very large transverse and longitudinal accelerator acceptances. The above requirement drives the design to low RF frequency, e.g. 200 MHz. If normal-conducting cavities at that frequency were used, the required high gradients would demand unachievably high peak power RF sources. The RF power can then be delivered to the cavities over an extended time, and thus RF source peak power can be reduced.

A conceptual design of an RLA based muon accelerator complex is presented. The scheme involves three superconducting linacs (200 MHz): a single pass linear Pre-accelerator followed by a pair of multi-pass 'Dogbone' recirculating linacs (RLA). In the presented scenario, acceleration starts after ionization cooling at 273 MeV/c and proceeds to 12.6 GeV, where the beam may be injected into an FFAG ring for further acceleration. The Pre-accelerator captures a large muon phase space coming from the cooling channel. It accelerates muons to relativistic energies, while adiabatically decreasing the phase-space volume, so that effective acceleration in recirculating linacs is possible. The 'Dogbone' RLAs further compress and shape-up the longitudinal and transverse phase-spaces, while increasing the energy. The proposed 'Dogbone' RLA configuration facilitates simultaneous acceleration of both μ^+ and μ^- species through the requirement of mirror symmetric optics of the return 'droplette' arcs.

For these studies, the transverse normalized acceptance (defined as $2.5\sigma_{rms}$) is chosen to be 30 mm-rad, and the longitudinal normalized acceptance is 150 mm-rad [3]. The transverse and longitudinal normalized acceptance is defined in Table 1, where p is the total momentum, m_μ is the muon mass, and c is the speed of light.

Normalized Emittances:		ε_{rms}	$A = (2.5)^2\ \varepsilon$
transverse emittance: $\varepsilon_x/\varepsilon_y$	mm·rad	**4.8**	**30**
longitudinal emittance: ε_l ($\varepsilon_l = \sigma_{\Delta p}\ \sigma_z/m_\mu c$) momentum spread: $\sigma_{\Delta p/p}$ bunch length: σ_z	mm mm	**27** **0.07** **176**	**150** **±0.17** **±442**

Table1. Beam emittance/acceptance after the cooling channel at 273 MeV/c.

'Racetrack' vs. 'Dogbone' RLA Configurations

As illustrated in Figure 1, most of the performance merits of the 'Racetrack' and 'Dogbone' RLA configurations with the same number of passes and the same net linac length, such us: the ratio of arc-to-linac beamline length, top-to-injection focusing mismatch in the linacs, etc, are quite comparable. Slightly more efficient use of the RF in the Dogbone results from injecting muons into the 'Dogbone' at the middle of the linac, which offers an additional 'half-pass' of acceleration through the RLA.

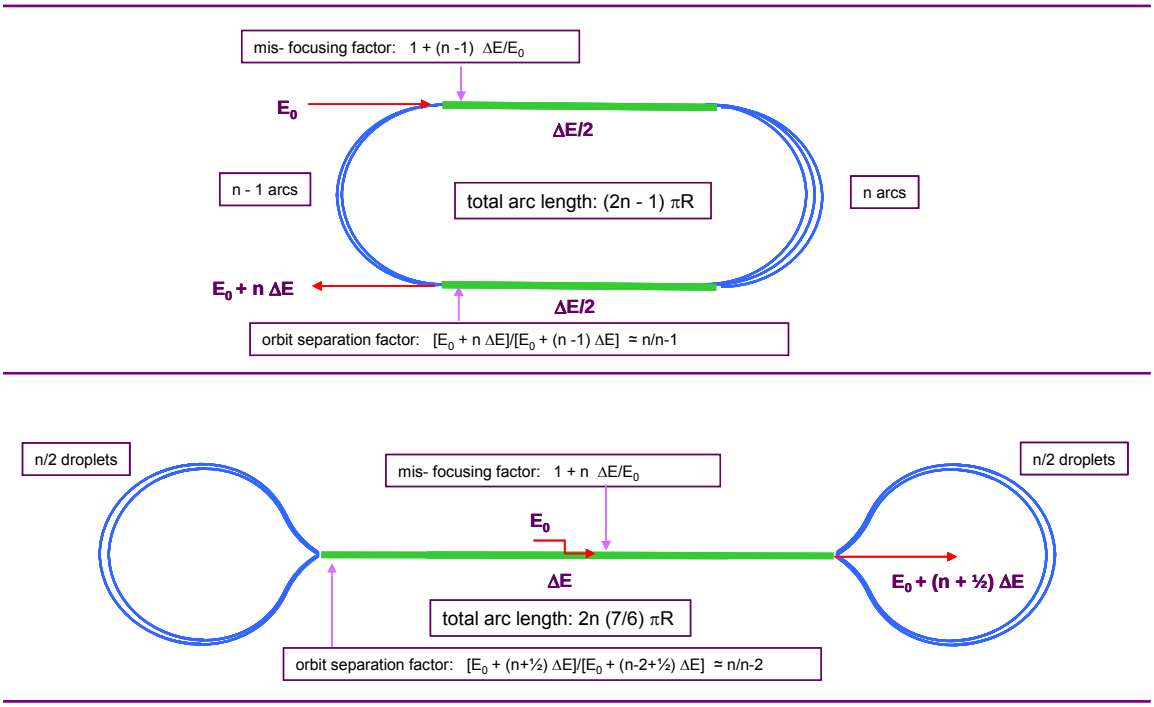

Figure 1. Performance merits of the 'Racetrack' and 'Dogbone' RLA configurations

However, there are two notable advantages of the 'Dogbone' configuration compared to the 'Racetrack':

- Better orbit separation at the linac ends resulting from larger (factor of two) energy difference between two consecutive linac passes for the 'Dogbone'
- Optimum optics solution for simultaneous acceleration of both muon species, μ^+ and μ^-, can be supported by the 'Dogbone topology', which allows both charge species to traverse the linac in the same direction (more uniform focusing profile) while passing in the opposite directions through the 'droplette' arcs.

12 GeV Two-step-Dogbone RLA

Here, we propose the 'baseline' acceleration scheme consisting of a linear Pre-accelerator and two 4.5 pass Dogbone RLAs, which simultaneously accelerate both $\mu^\pm$ species from about 0.3 GeV (after the cooling channel) to 12.6 GeV. The acceleration complex is illustrated schematically in Figure 2.

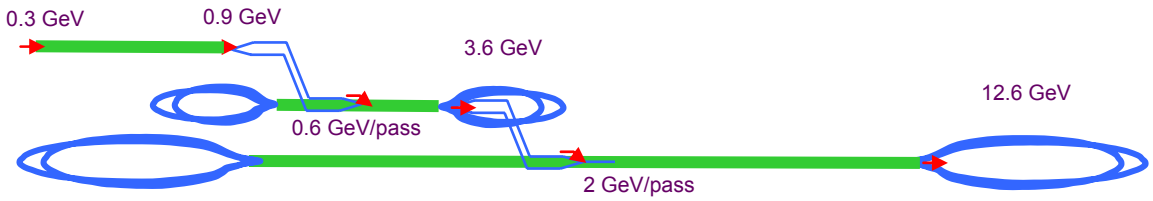

Figure 2. Layout of a two-step-Dogbone RLA complex. For compactness all there components (Pre-accelerator, Dogbone I and Dogbone II) are stacked up vertically; $\mu^\pm$ beam transfer between the accelerator components is facilitated by the vertical double chicane (to be described later)

Selection of higher number of passes in each RLA (4.5 vs 3.5 in Study 2a) for the baseline scheme, is driven by recent successful studies of FODO based lattices, which are more suitable (compared to the Triplet focusing) to accommodate large number of passes in a 'Dogbone' configuration. The new focusing structure (to be described later in this study) offers a well balanced multi-pass linac optics as well as uniform beta matching to the 'droplette' Arcs. Furthermore, the FODO structure can still support a compact Spreader/Recombiner optics and a uniform dispersion flip for the 'droplette' Arcs, as will be illustrated with specific lattices at the end of this study.

The energy range for each 'Dogbone' RLA was chosen to give similar ratios of top-to-injection energies: namely 3.5 for Dogbone I and 4.0 for Dogbone II. Furthermore, the injection energies for both RLAs were chosen, so that a tolerable level of the RF phases slippage along a

given length linac can be maintained. A simple calculation of the phase slippage of a muon injected with the initial energy E_0 and accelerated by ΔE in a linac of length, L, where uniformly spaced RF cavities are phased for the speed-of-light particle was carried out using the following cavity-to-cavity iterative algorithm for phase-energy vector:

$$\begin{pmatrix} \phi b_{k,i+1} \\ Eb_{k,i+1} \end{pmatrix} := \begin{bmatrix} \phi b_{k,i} + \frac{h}{\lambda} \cdot 360 \cdot \left[\frac{1}{2} \cdot \left(\frac{m_\mu}{Eb_{k,i}} \right)^2 \right] \\ Eb_{k,i} + h \cdot \Delta E_k \end{bmatrix}$$

where

$$h := \frac{L_{linac}}{N_{cav}} \qquad \lambda := \frac{c}{f_0} \qquad k := 0..4 \qquad i := 0..1N_{cav} - 1$$

The resulting phase slippage profile along the multi-pass linacs is illustrated in Figure 3 for both Dogbone I and II. The injection energy to Dogbone I set at 0.9 GeV results in still manageable phase slip of about 40 deg. for the initial 'half-pass' through the linac. The corresponding value of phase slip for Dogbone II is much lower, about 10 deg.

Dogbone I

$E_0 = 0.9GeV$, $\Delta E = 0.6GeV$, $L = 70m$

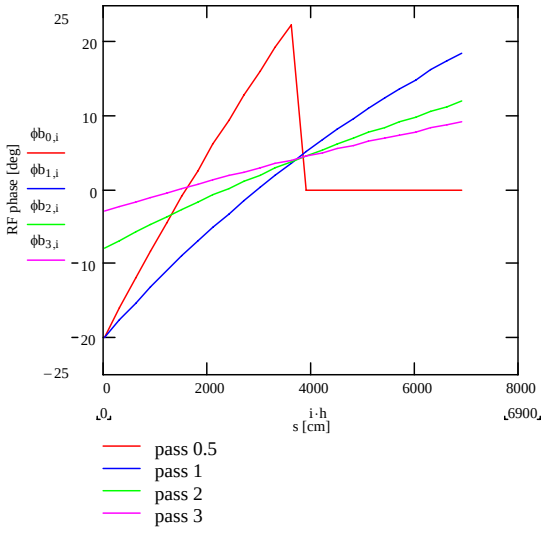

$\phi b_{0,0} := -20$ $\phi b_{1,0} := -20$

$\phi b_{2,0} := -8$ $\phi b_{3,0} := -3$

Dogbone II

$E_0 = 3.6GeV$ $\Delta E = 2GeV$ $L = 240m$

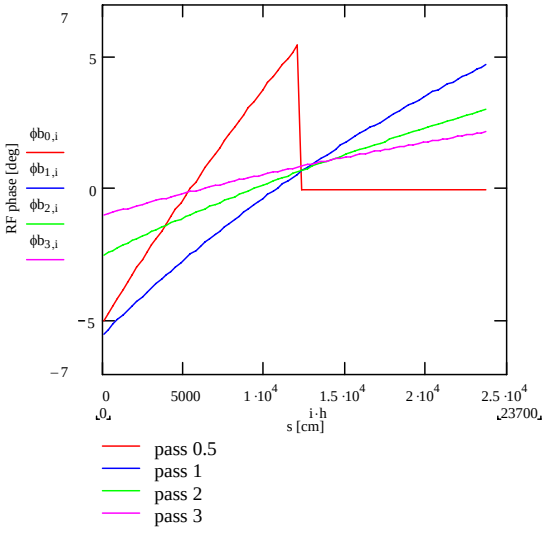

$\phi b_{0,0} := -5$ $\phi b_{1,0} := -5.5$

$\phi b_{2,0} := -2.5$ $\phi b_{3,0} := -1$

Figure 3. RF phase slippage along the multi-pass linacs; initial 'gang phases' for each pass (listed at the bottom of the plots in the RF degrees) were chosen for the optimum longitudinal bunch compression in each linac-Arc segment.

Initial bunch length and energy spread are still too large at the RLA input and further compression is required in the course of acceleration. To accomplish that, the beam is accelerated off-crest with non zero M_{56} (momentum compaction) in the 'droplette' Arcs [1]. This induces synchrotron motion, which suppresses the longitudinal emittance growth related to non-linearity of accelerating voltage. Without synchrotron motion the minimum beam energy spread would be determined by non-linearity of RF voltage at bunch length and would be equal to $(1-\cos\phi) \approx 9\%$ for bunch length ϕ=30 deg. The synchrotron motion within the bunch averages the total energy gain of tail's particle to the energy gain of particles in the core. It was chosen to have the same values of M_{56} for all 'droplette' Arcs - the optimum value is about about 5 m, while optimal detuning of RF phase from on-crest position is different for different arcs (see 'gang phases' for various passes listed in Figure 3).

Linear Pre-Accelerator

The initial longitudinal acceptance of the linear accelerator is chosen to be 2.5σ, i.e. $\Delta p/p=\pm 17\%$ and RF pulse length $\Delta\phi=\pm 73$ deg. To perform adiabatic bunching [1], the RF phase of the cavities is shifted by 72 deg at the beginning of the pre-accelerator and gradually changed to zero by the linac end. In the first half of the linac, when the beam is still not sufficiently relativistic, the offset causes synchrotron motion, allowing bunch compression in both length and momentum spread to $\Delta p/p=\pm 7\%$ and $\Delta\phi=\pm 29$ deg. The synchrotron motion also suppresses the sag in acceleration for the bunch head and tail. Figure 4 shows how the initially elliptical boundary of the bunch longitudinal phase space will be transformed by the end of the linac.

Particle distribution for tracking has been chosen to be Gaussian in 6D phase space but the tails of the distribution are truncated at 2.5σ, which corresponds to the beam acceptance presented in Table 1. Despite the large initial energy spread, particle tracking through the linac does not exhibit any significant emittance growth with 0.2% beam loss coming mainly from particles at the longitudinal phase space boundary. Figure 5 shows the beam envelopes along the linac as well 'snapshots' of the longitudinal phase space at the beginning, middle and the end of the Pre-accelerator. Sudden increase and then decrease of the envelopes correspond to a particle motion instability with consequitive particle scraping..

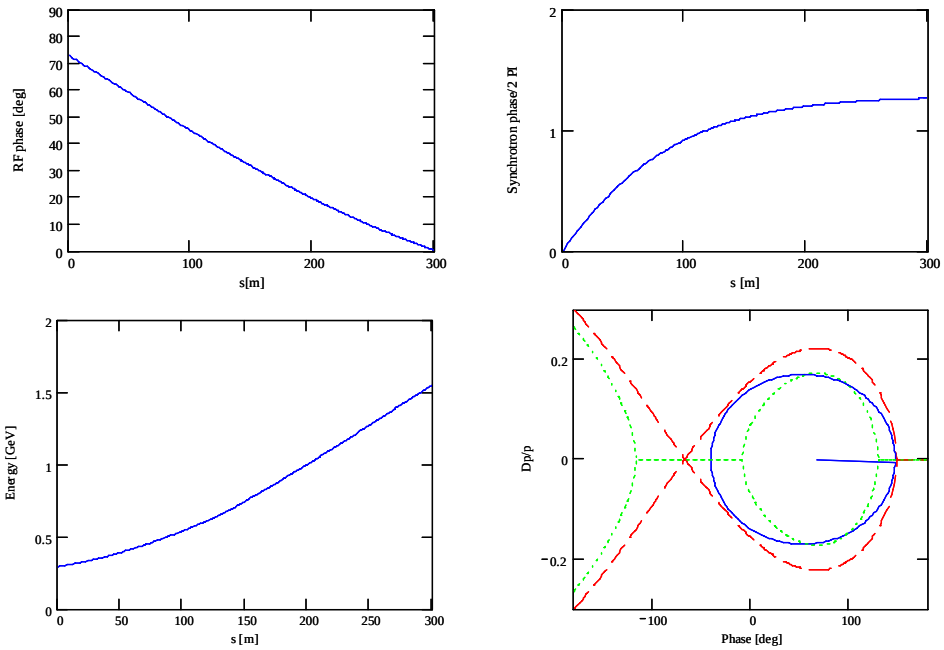

Figure 4. .Individual cavity phasing along the linac and the resulting synchrotron motion. Energy profile and the longitudinal beam boundary (solid line) inside a separatrix (dashed line) shown at the beginning of the linac ($\Delta p/p=\pm 0.18$ or $\Delta\phi=\pm 73$deg.)

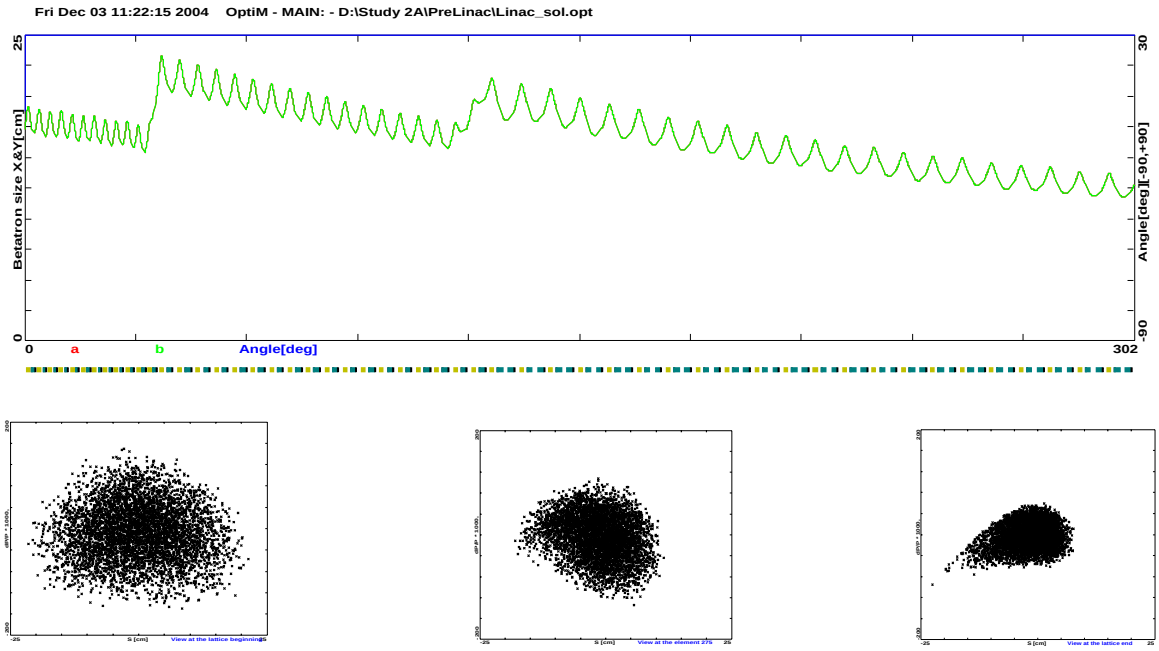

Figure 5. Top, transverse beam envelopes in the Pre-Accelerator linac – uniform periodic focusing with three styles of cryo-modules. Below, longitudinal phase-space: before, half-way through and at the end of acceleration, as illustrated by particle tracking

Multi-pass Linac Optics – FODO vs Triplet Focusing

Two styles of focusing (FODO and Triplet) were considered as a base for building RLA lattices. The requirement of quasi-periodic focusing throughout the entire beamline imposes consistent use of one of the styles for all lattice segments (multi-pass linac and recirculation Arcs). Specific features (advantages and disadvantages) of both style focusing are summarized in Figure 6

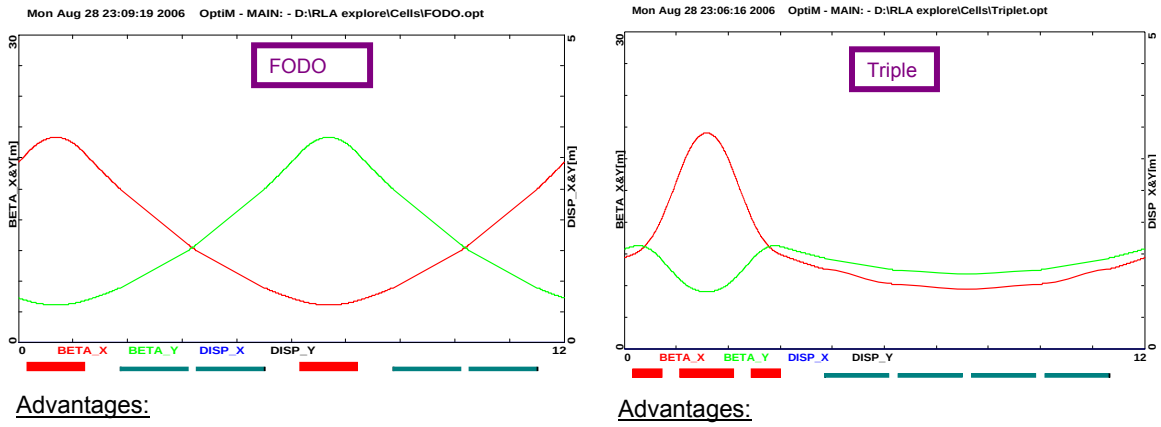

Advantages:

- much weaker quads (~3 times)
- shorter quads (total)
- easier chromaticity correction

Advantages:

- longer straight sections
- smaller vertical beta-function
- uniform variation of betas

Figure 6. FODO vs. Triplet focusing structure – Comparison of same length periodic cells (90 deg. betatron phase advance per cell)

The key element of the transverse beam dynamics in a multi-pass 'Dogbone' RLA is an appropriate choice of multi-pass linac optics. The focusing profile along the linac (quadrupole gradients) need to be set (and they stay constant), so that one can transport (provide adequate transverse focusing for given aperture) multiple pass beams within a vast energy range. Obviously, one would like to optimize the focusing profile to accommodate maximum number of passes through the RLA. In addition, the requirement of simultaneous acceleration of both $\mu^{\pm}$ species imposes mirror symmetry of the 'droplette' Arcs optics (the two species move in the opposite directions through the Arcs). This in turn puts a constraint on the exit/entrance Twiss functions for the two consecutive linac passes, namely $\beta_{out}^{n} = \beta_{in}^{n+1}$ and $\alpha_{out}^{n} = -\alpha_{in}^{n+1}$, where n = 0, 1, 2.. is the pass index.

We will examine the two styles of focusing (Triplet and FODO) to design the optimum multi-pass linac optics for the 'Dogbone' RLA. The example presented below describes a 'Dogbone'

based on a 2 GeV per pass linac (240 m long) with the injection energy of 2 GeV. Since the beam is traversing the linac in both directions throughout the course of acceleration one chooses a ‘flat’ focusing profile for the entire linac: e.g. the quads in all cells are set to the same gradient, corresponding to 90 deg. phase advance per cell determined for the lowest (injection) energy – no scaling up with energy for the quad gradients along the linac.

Figure 7 and 8 illustrate multi pass optics for the Triplet and FODO based linacs. One can see immediately superiority of the FODO structure, which supports twice as many passes through the ‘Dogbone’ RLA (6 vs. 3 passes).

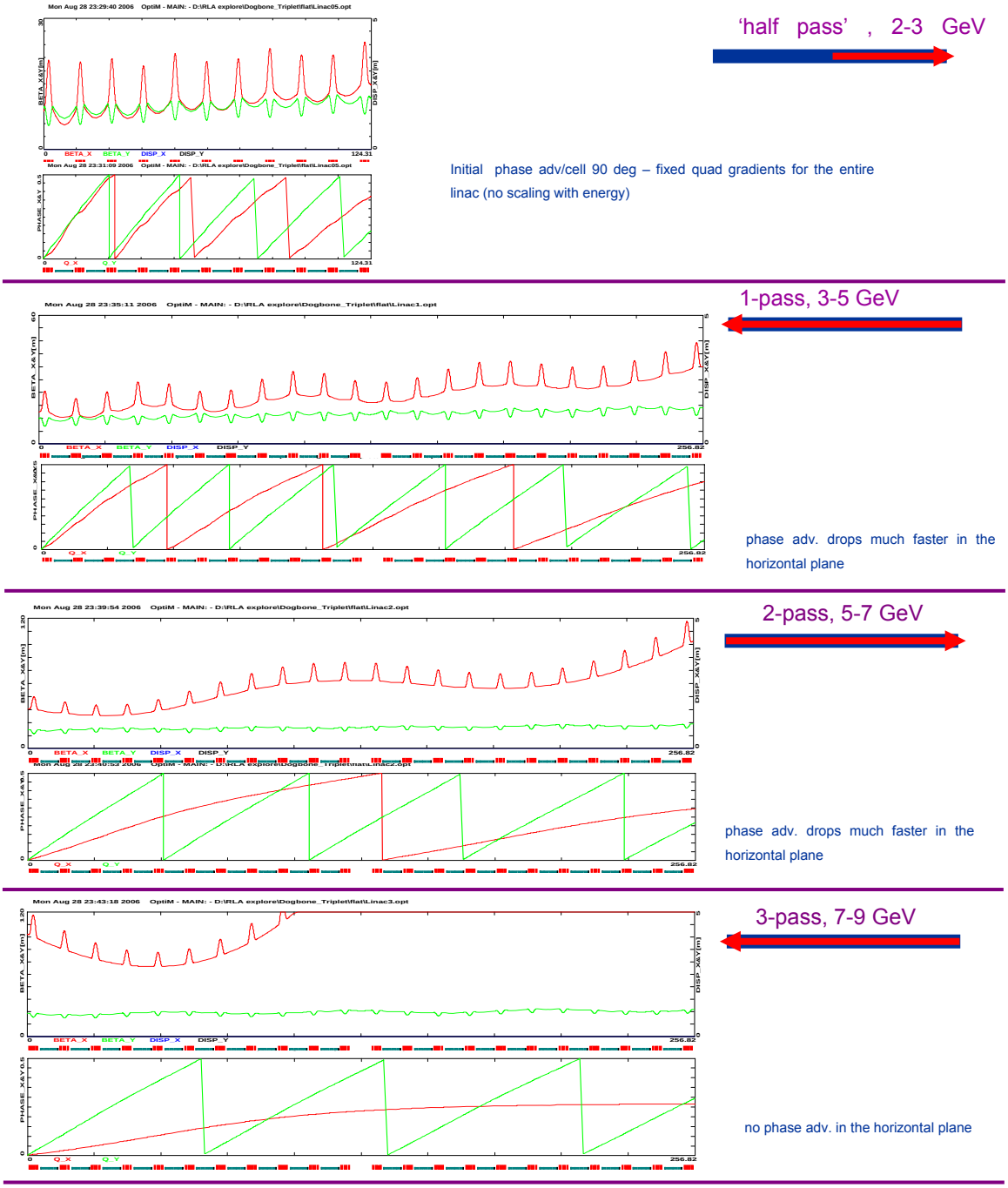

Figure 7. Triplet based multi-pass linac optics – quadrupoles in all cells are set to the same gradient, corresponding to 90 deg. phase advance per cell at 2 GeV. Inherent to the triplet focusing asymmetry between the horizontal and vertical planes (middle quad focusing horizontally, outer quads focusing vertically) manifests itself via rapid phase advance loss in the horizontal plane for higher passes; already at third pass energy the horizontal focusing is almost lost resulting in catastrophic beam blowup.

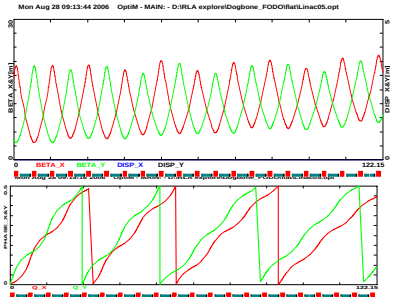

'half pass', 2-3 GeV

initial phase adv/cell 90 deg – fixed gradient in all cells (no scaling with energy)

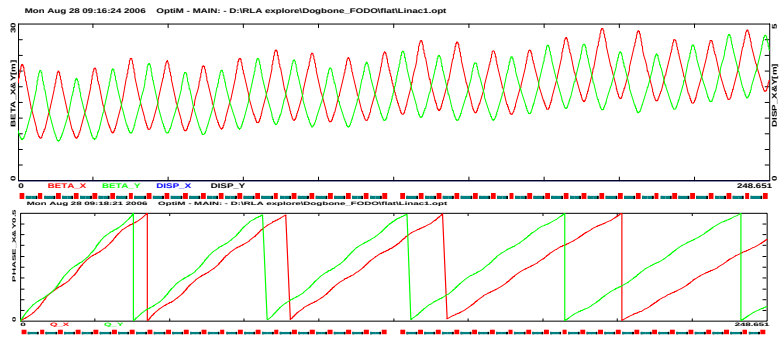

1-pass, 3-5 GeV

phase adv. diminish uniformly in both planes

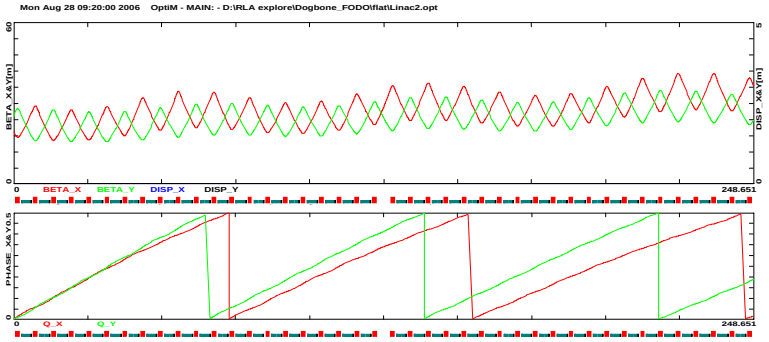

2-pass, 5-7 GeV

phase adv. diminish uniformly in both planes

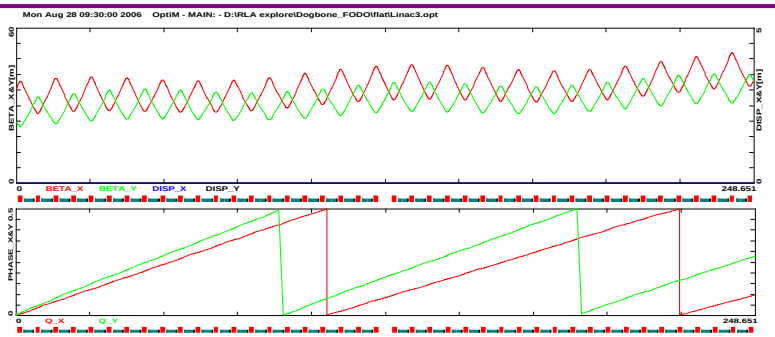

3-pass, 7-9 GeV

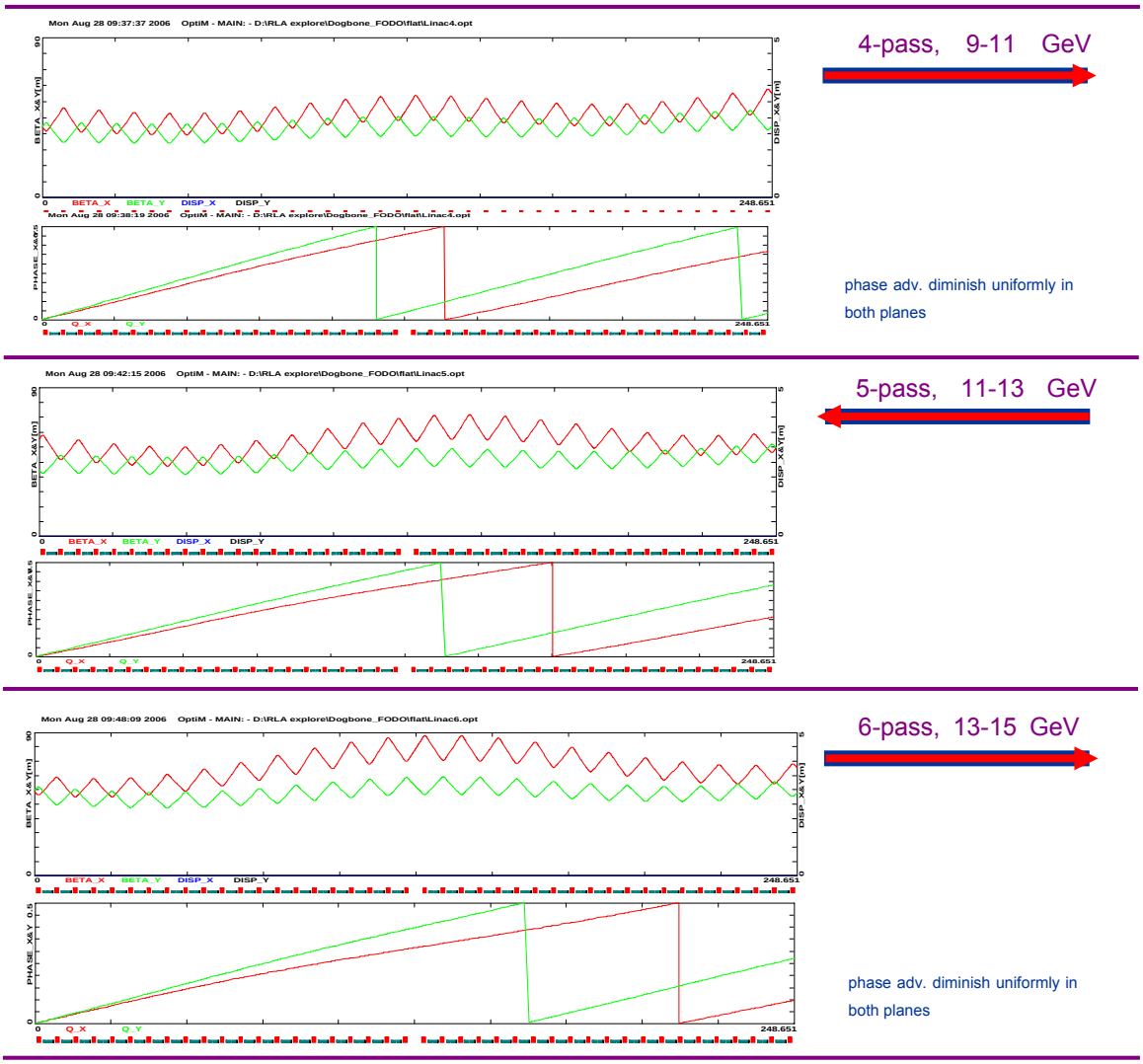

Figure 8. FODO based multi-pass linac optics – quads in all cells are set to the same gradient, corresponding to 90 deg. phase advance per cell at 2 GeV. Inherent to the FODO focusing symmetry between the horizontal and vertical planes – betatron phase advance gradually diminish uniformly in both planes. The resulting linac optics is well balanced in terms of Twiss functions and beam envelopes; there is sufficient phase advance up to 6-th pass.

Encouraged by the above 6-pass linac optics one could consider a more aggressive 6.5-pass 15 GeV 'Dodbone' RLA based on 2 GeV/pass linac, with the top-to-injection energy ratio of 7.5. Its layout is illustrated in Figure 9. Furthermore, orbit separation on a single dipole magnet for multi-pass energies seems quite feasible for the above scheme (see Figure 10).

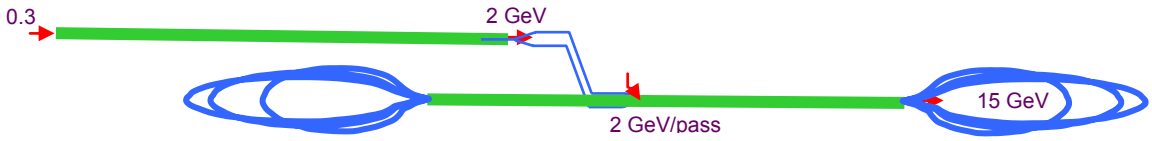

Figure 9. Layout of a 6.5-pass 'Dogbone' RLA complex; including a 2 GeV Pre-accelerator and 2-to-15 GeV 'Dogbone' RLA based on 2 GeV/pass linac

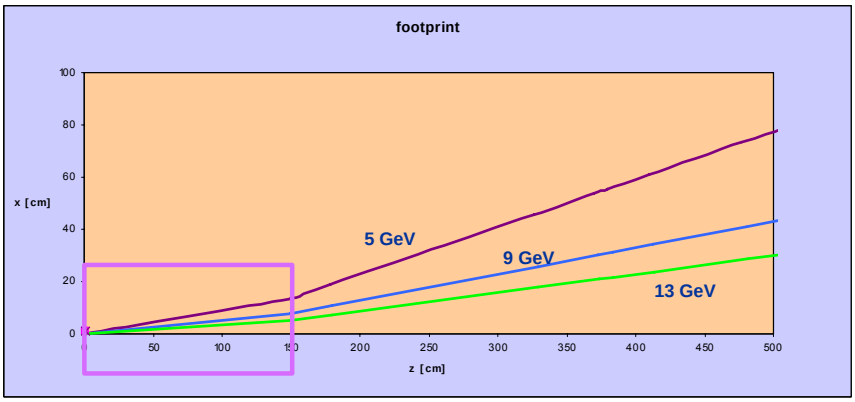

Figure 10. End-of-linac orbit separation (single dipole) for multi-pass beams with increasing energies

'Droplette' Arcs

In a 'Dogbone' RLA one needs to separate different energy beams coming out of a linac and to direct them into appropriate 'droplette' arcs for recirculation [4]. For multiple practical reasons horizontal rather than vertical beam separation was chosen. Rather than suppressing horizontal dispersion created by the Spreader it is smoothly matched to the horizontal dispersion of the outward 60 deg. arc. Then by appropriate pattern of removed dipoles in three transition cells one 'flips' the dispersion for the inward bending 300 deg arc, etc. The entire 'droplette' Arc architecture is based on 90 deg. phase advance cells with periodic beta functions. The lattice building blocks along with the 'droplette' Arc footprint are illustrated in Figure 11.

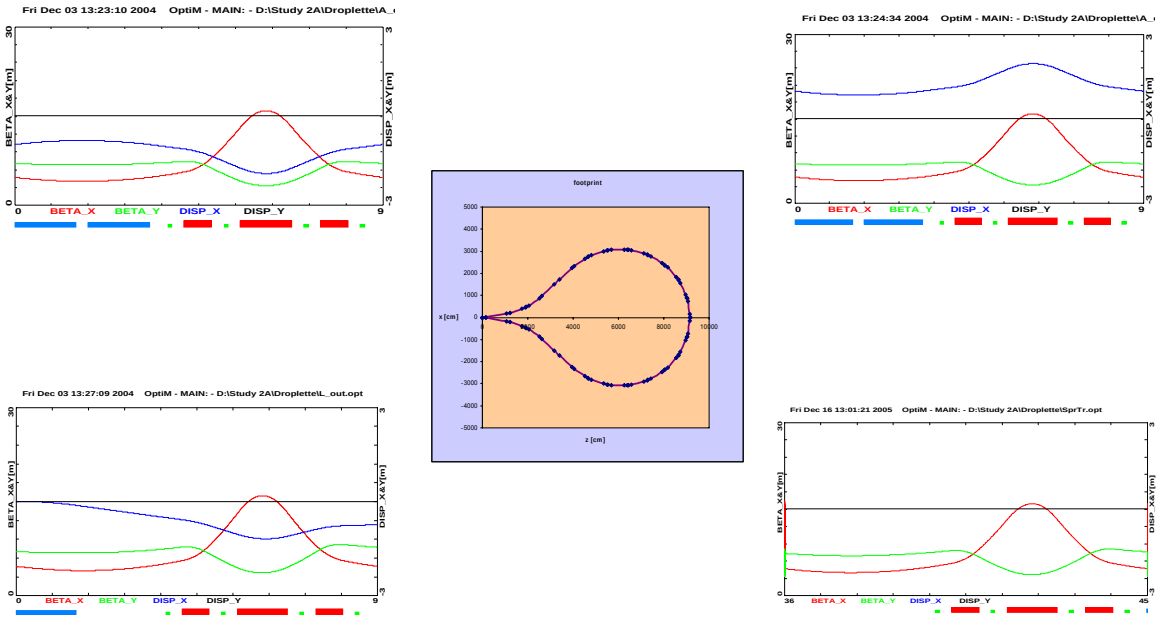

Figure 11 The lattice building blocks – Triplet 90^0 phase advance/cell: inward and outward cells, missing dipole, empty cells.

The resulting 'droplette' Arc optics based on Triplet focusing [4] is illustrated in Figure 12. One can easily estimate the momentum compaction of the 'droplette' Arc as follows:

$$M_{56} = -\int \frac{D_x}{\rho} ds = -D_x^{dip} \int d\left(\frac{s}{\rho}\right) = -D_x^{dip} \int d\theta_{rad} = -D_x^{dip} \times \theta_{rad}^{tot}$$

$$M_{56} = -\frac{5}{3}\pi \times 1.2\ m = -6.3\ m$$

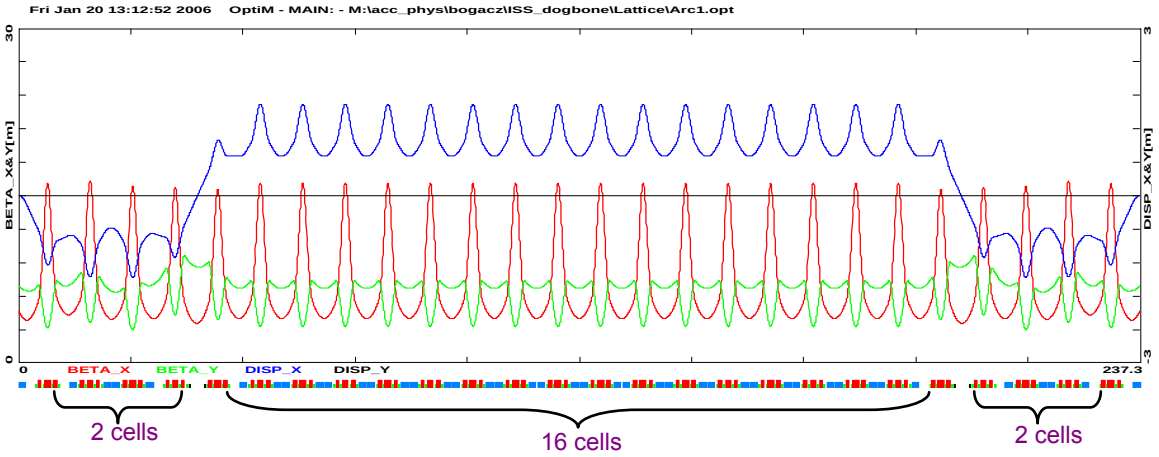

Figure 12 'Droplette' Arc optics – uniform periodicity of beta functions and dispersion

Similarly one can design ‘droplette’ Arc optics analogous to the one illustrated in Figure 12 using FODO cells as the basic building blocks. The spreader optics for both styles of focusing is illustrated in Figure 13.

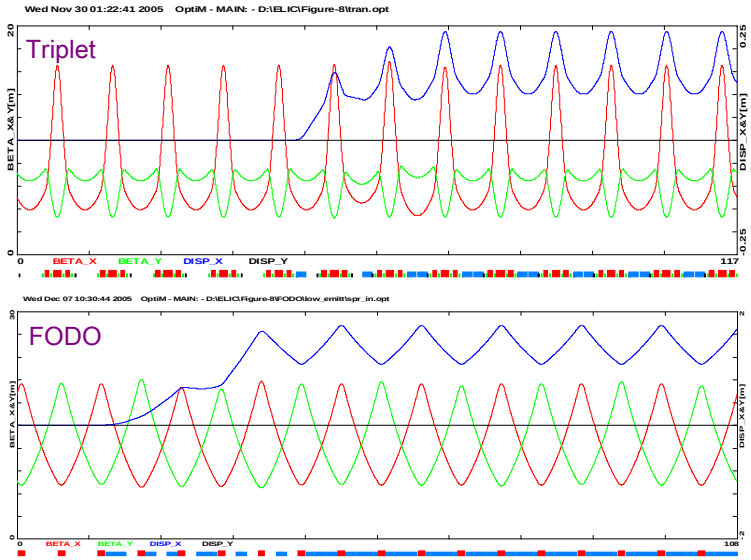

Figure 13 Spreader optics (Triplet and FODO) – uniform periodicity of beta functions and dispersion.

Injection Double Chicane

To transfer both $\mu^{\pm}$ species from one accelerator to the other one located at a different vertical elevation one can design a compact double chicane based on a periodic 90 deg. phase advance cell (in either Triplet of FODO style). Each ‘leg’ of the chicane involves 4 horizontal and 2 vertical bending magnets, forming a double achromat in the horizontal and vertical planes, while preserving periodicity of beta functions. The layout and Twiss functions of the double chicane are illustrated in Figure 14.

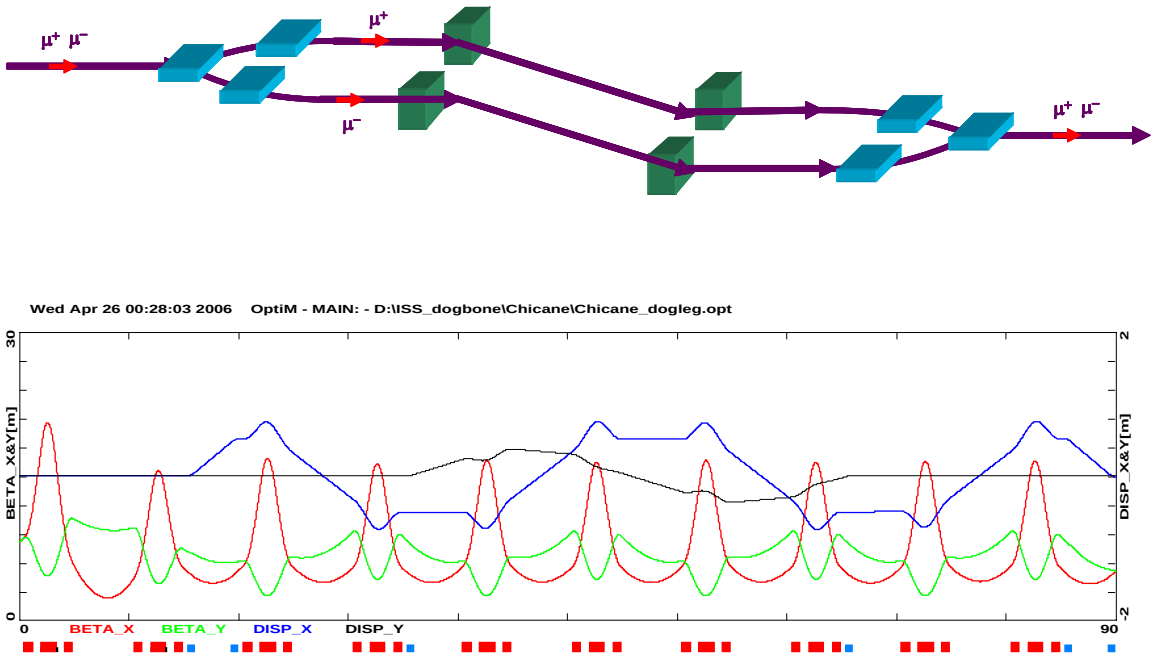

Figure 14. Layout and optics of the Injection Double Chicane

Magnet Error Tolerances

Presented lattices, linacs and 'droplette' Arcs were checked for error sensitivities. First, lattice sensitivity to random misalignment errors was studied for a 'droplette' Arc via DIMAD Monte-Carlo assuming 1 mm (sigma rms) quad misalignment in x and y. The resulting orbit deviation is illustrated in Figure 15.

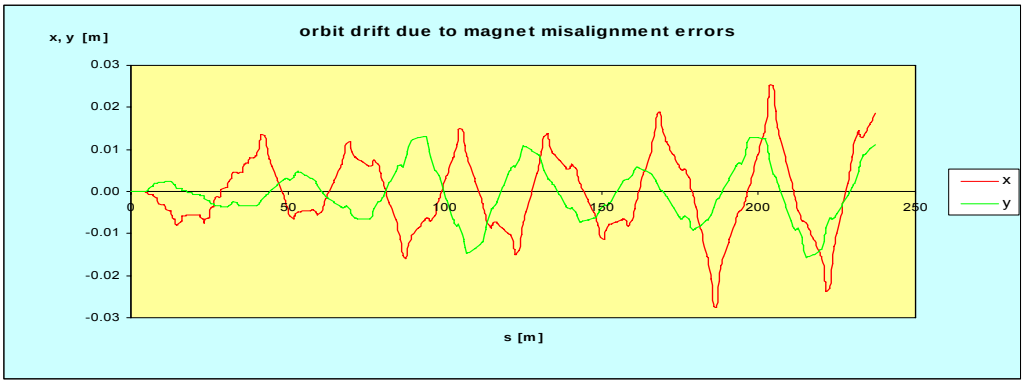

Figure 15 Orbit drift due to magnet misalignment errors – a few mm per cell

The level of a few mm orbit drift between adjacent cells can easily be corrected by a pair of 2000 Gauss cm correctors located at every girder.

Furthermore, the lattices were tested for magnet field error tolerance, as follows. By design, one can tolerate some level (e.g. 10%) of Arc-to-Arc betatron mismatch due to the focusing errors, $\delta\phi_1$ (quad gradient errors and dipole body gradient) to be compensated by the dedicated matching quads.

$$\left(\frac{\sigma_\varepsilon}{\varepsilon}\right)_{mis} = \sqrt{\frac{1}{2}\sum_{n=1}^{N}\left(\beta_n \delta\phi_1\right)^2} = \sqrt{\frac{1}{2}\Delta\phi_1^2\sum_{n=1}^{N}\left(\beta_n\right)^2_{quad} + \frac{1}{2}\delta\phi_1^2\sum_{n=1}^{N}\left(\beta_n\right)^2_{dipole}}$$

The resulting focusing error tolerance evaluated for Arc 2 – linac 2 lattice segment from the above formula (summation of beta squares for the lattice) is illustrated in Figure 16.

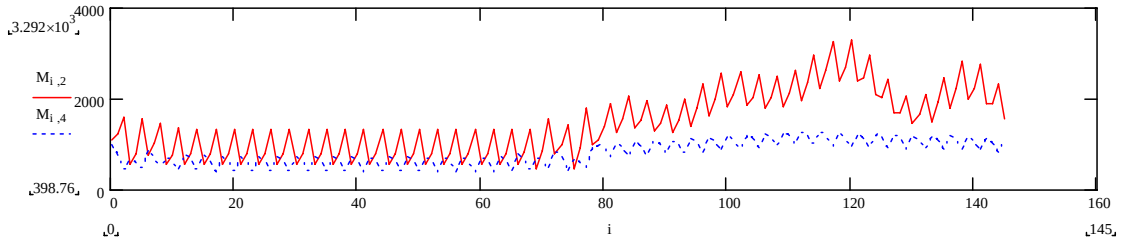

F_{min} = 1.5 m (GdL=65 kG)

$$\sqrt{\frac{1}{2F_{min}^2}\sum_{n=1}^{N}\beta_n^2} \simeq 190$$

$$\frac{\Phi}{\phi_1^{max}} = 0.001$$

$$\Phi = \sqrt{\delta\phi_1^2 + \frac{3}{2}a^2\left(\delta\phi_2^2 + 2\delta\phi_1\delta\phi_3\right) + \frac{5}{2}a^4\left(\delta\phi_3^2 + 2\delta\phi_1\delta\phi_5 + 2\delta\phi_2\delta\phi_4\right) + \ldots}$$

Figure 16 Focusing errors tolerance for the presented lattice – 10% of Arc-to-Arc betatron mismatch limit sets the quadrupole field spec at 0.1% (including all higher multipoles).

Summary

Results of this study suggest that there are no obvious physical or technical limitations precluding design and construction of a 'Dogbone' RLA for acceleration of muons to 12.5 GeV and beyond. Design choices made in the proposed acceleration scheme were driven by the beam dynamics of large phase-space beams.

The 'Dogbone' configuration was chosen (rather than the 'Racetrack') because of better orbit separation at the linac ends and simpler optics solution for simultaneous acceleration of both muon species, μ^+ and μ^- that can be supported by the 'Dogbone topology' (allowing both charge species to traverse the linac in the same direction).

The FODO based lattices were found more suitable (compared to the Triplet) to accommodate large number of passes in a 'Dogbone' RLA. The FODO structures offer well balanced multi-pass linac optics, as well as uniform beta matching to the 'droplette' Arcs. Furthermore, it can still support a compact Spreader/Recombiner optics and a uniform dispersion flip for the 'droplette' Arcs.

Presented lattices were checked for error sensitivities: random misalignment errors and magnet field error tolerances. The results were very encouraging: the orbit drift due to the magnet misalignment errors was confined to just a few mm per cell (easily correctable by a pair of standard correctors) and the focusing errors tolerance turned out very high – 10% of Arc-to-Arc betatron mismatch allowance sets the quadrupole field quality spec at 0.1% (including all higher multipoles).

In conclusion, the proposed acceleration and beam transport scheme is well suited for handling large phase space beams.

References

1 S.A. Bogacz, Journal of Physics G: Nuclear and Particle Physics, **29**, 1723, (2003)

2. J.S. Berg et al., Physical Review Special Topics – Accelerators and Beams, **9**, 011001 (2006)

3 S.A. Bogacz, Nuclear Physics B, Vol **149**, 309, (2005)

4 S.A. Bogacz, Nuclear Physics B, Vol **155**, 334, (2006)